

Paracrine regulated protective mechanisms in the organ of Corti

PhD Thesis



Tamás Horváth M.D.

Semmelweis University
Szentágothai János Doctoral School of Neurosciences
Program: Functional Neuroscience
Program Director: Prof. Dr. Szilveszter Vizi E., D.Sc.

Tutor: Dr. Tibor Zelles, PhD.

Opponents: Dr. Ákos Zsembery, PhD.
Dr. Frigyes Helfferich, PhD.

Examination Committee:

President: Prof. Dr. Éva Szökő, D.Sc.

Members: Dr. Marianna Küstel, Ph.D.
Dr. Andor Hirschberg, Ph.D.

Budapest
2016

1 INTRODUCTION

General considerations

Hearing loss is the most common human sensory deficit affecting more than 360 million people worldwide, due to the aging society, the increasing noise exposure, but ototoxicity and genetical hearing loss also play a role. Impairments of the cochlea or the auditory nerve, i.e., sensorineural hearing losses (SNHLs; e.g., noise-induced hearing loss or presbycusis) are not curable by pharmacological tools. Although there are many evidences about the underlying mechanisms, the unique anatomy and physiology of the cochlea and especially of the organ of Corti -that amplifies the mechanical soundwaves and converts them into electrical signals- hampers observing the function of the inner ear. However, there are endogenous protective mechanisms in the cochlea. Attenuation of cochlear amplification and decrease in the efficiency of the inner hair cell (IHC)-auditory nerve transmission provides protection of hearing. Unmapping these functions can facilitate to find effective medical treatment or prevention for SNHL. In our study, we examined two different paracrine regulated signaling mechanisms in the organ of Corti that are supposed to play a role in hearing protection.

Protective regulation of the cochlear amplification: purinergic Ca^{2+} signaling in the supporting cells of the organ of Corti

The passive sound waves are actively amplified in the organ of Corti by the outer hair cells that are surrounded by the glia-like network of supporting cells. Supporting cells supposed to help maintaining cochlear homeostasis and also play an important active role in normal functions and pathological processes in hearing. There are protective mechanisms that are regulating cochlear amplification by adenosine-triphosphate (ATP), that evoke intra- and intercellular Ca^{2+} signals. ATP is released into the endolymph from the stria vascularis, and its concentration elevates during noise exposure,

inducing K^+ shunting from the endolymph by activating P2 receptors on the apical surface on the cells that are lining the endolymphatic space. This results in a reduction of the endocochlear potential as a protection against over-amplification. Besides this, the supporting cells themselves are able to release ATP into the extracellular space through connexin hemichannels, and ATP can also escape from injured hair cells, inducing intercellular Ca^{2+} waves among the supporting cells as sensing the damage.

Although purinergic signaling in the different types of supporting cells have been previously studied, those experiments were largely performed on isolated cells or tissue culture, or in embryonal and neonatal tissue. There is a need for a method that is more close to the in vivo situation to observe ATP-evoked Ca^{2+} signaling parallel, in situ, in supporting cells of hearing animal.

Dopaminergic lateral olivocochlear efferents

Glutamate is the neurotransmitter of the inner hair cells that activates the afferent hearing nerve. It is known that dopamine- (DA) containing boutons of the lateral olivocochlear (LOC) efferent fibers have axo-dendritic synapses on afferent dendrites and modulate afferent neurotransmission, and several lines of evidence suggest that DA may have a protective effect on cochlear function. All types of ionotropic glutamate receptors have been identified on afferent dendrites. The clinical importance of glutamate receptors has been highlighted by the finding that N-methyl-D-aspartate (NMDA) and AMPA receptors play an important role in the development of cochlear damage. Extreme glutamate levels cause excessive Na^+ and Ca^{2+} fluxes through AMPA and NMDA receptors in afferent dendrites in turn leading to water influx and swelling, and Ca^{2+} can activate proteases and lipases that lead to the irreversible damage of the cells. The increased Ca^{2+} level becomes sufficient to activate the nitric oxide synthase (NOS) that is linked to NMDA receptors. The neuronal form of NOS is connected to NMDA receptors and produces NO primarily in response to the activation of NMDA receptors, and can act on nonsynaptic targets, and interacts with the DA release in the striatum. Different NOS isoforms were identified

in the organ of Corti, and significant NO activity was reported in the cochlea. It has also been suggested that NO in the human cochlea could act as a neurotransmitter/neuromodulator. Although several aspects of NO as a transmitter have been described in the cochlea, very little is known about the role of NO in modulating the release of cochlear neurotransmitters.

2 SPECIFIC AIMS

Purinergic Ca²⁺ signaling in the supporting cells of the organ of Corti

- Creating a functional Ca²⁺ imaging model based on the acute hemicochlea preparation of hearing mice in which purinergic Ca²⁺ signaling can be measured parallel in different types of supporting cells of the organ of Corti
- Characterizing the ATP-evoked Ca²⁺ signaling in three different supporting cell types (pillar-, Deiters-, and Hensen cells) in terms of reversibility, repeatability, dose-dependency, and desensitization
- Evaluating the role of the extracellular Ca²⁺ and intracellular Ca²⁺ stores in the ATP-evoked Ca²⁺ signaling
- Determining the differences in the ATP-evoked Ca²⁺ signaling in the different types of supporting cells

The role of NO and NMDA receptors in DA release from the LOC efferents

- Exploring the local DA releasing effect of NO and the ionotropic glutamate receptors NMDA
- Uncovering the regulatory mechanism behind the effect of NO and NMDA receptors on cochlear DA release

3 MATERIALS AND METHODS

Hemicochlea Ca²⁺ imaging

Tissue preparation:

Acutely dissected cochleae of P15-21 CD-1 mice were used. Following decapitation, bathed in artificial perilymph (in mM: NaCl 150; KCl 3.5; CaCl₂ 1; MgCl₂ 1; Hepes 7.75; Tris 2.25; glucose 5.55; pH 7.4; 320 mOsm/l), gassed with O₂, one of the bullas was removed, the cochlea was exposed, glued onto a plastic plate, and cut into half through the middle of the modiolum.

Ca²⁺ imaging:

Hemicochleae were incubated with the Ca²⁺ dye fura-2 AM (10 μM) in the presence of pluronic F-127 (0.05%, w/v) for 30 min, then deesterified before recording. The fura-2 loaded hemicochlea was alternately illuminated by 340 ± 5 nm and 380 ± 5 nm excitation light during imaging. The emitted light was monitored after passage through a 510-nm cut-off filter (20 nm band-pass). We imaged supporting cells in the basal turn of the cochlea throughout this study, and cells in 1-3 layers down the cut surface of the hemicochlea were used. Integrity of the preparations was assessed by the gross anatomy, the shape and location of the cells, the basal-, tectorial- and the Reissner's membranes and only the intact hemicochleae were used.

Drug delivery:

ATP was added to the perfusion for 30 sec. Cyclopiazonic acid (CPA) and PPADS were present in the perfusion during the 2nd ATP administration in the appropriate experiments. Ca²⁺-free condition was achieved by the omission of Ca²⁺ from the buffer (+ 1 mM EGTA) with timing of application similar to CPA and PPADS application.

Data analysis:

The ratio of emitted fluorescence intensity (F₃₄₀ / F₃₈₀) was calculated and converted into absolute values of [Ca²⁺]_i. Cell image intensities were background-corrected using a nearby area devoid of loaded cells. Values of [Ca²⁺]_i in the cells were calculated off-line using the following equation: [Ca²⁺]_i = K_d x F_{max380} / F_{min380} x (R - R_{min}) / (R_{max} - R). Ca²⁺ transients were measured as the peak amplitude of ATP-evoked elevation of intracellular Ca²⁺

concentration ($\Delta[\text{Ca}^{2+}]_i$ in nM; peak - basal; basal means average baseline $[\text{Ca}^{2+}]_i$ obtained during a 30-60 sec period prior to the respective ATP stimulation). Effect of drugs, Ca^{2+} withdrawal, and desensitisation were expressed as the ratio of ATP response in the presence ($\Delta [\text{Ca}^{2+}]_{i,2}$) over the absence ($\Delta [\text{Ca}^{2+}]_{i,1}$) of the drug ($\Delta [\text{Ca}^{2+}]_{i,2} / \Delta [\text{Ca}^{2+}]_{i,1}$). Data are presented as mean \pm standard error of the mean (SEM). Number of experiments (n) shows the number of individual cells. Every treatment group had cells from at least four mice. One-way ANOVA with Bonferroni post hoc test were used to determine the significance of data. In the experiments analysing the effect of both repetition time of ATP application and cell type on desensitization two-way ANOVA followed by Bonferroni post hoc test was used. * $p < 0.05$, ** $p < 0.01$ or *** $p < 0.001$.

RT-PCR detection

Twenty CD-1 mice (P15-19) were decapitated, and the bullae were removed from the skull. The whole organ of Corti was removed from the bony modiolus, and the stria vascularis was peeled off, as well. The tissue was immediately collected into Eppendorf tubes cooled on dry ice, then stored at $-80\text{ }^\circ\text{C}$ till analysis. Total RNA from mouse cochlea samples was isolated with Trizol isolation reagent according to the protocol provided by the supplier. RNA ($2\mu\text{l}$) was reverse transcribed with RevertAid First Stand cDNA Synthesis Kit. Conditions for amplification: initial denaturation at $95\text{ }^\circ\text{C}$ for 5 min, hot start at $80\text{ }^\circ\text{C}$, then $94\text{ }^\circ\text{C}$ for 1 min, $59\text{ }^\circ\text{C}$ for 1 min, and $72\text{ }^\circ\text{C}$ for 1 min for 40 cycles, with a final extension at $72\text{ }^\circ\text{C}$ for 5 min. PCR products were analyzed by agarose gel electrophoresis.

In vitro measurement of DA released from LOC terminals

Animals and tissue preparation:

We used 15–25 g CD-1 male mice. After decapitating the animals, the cochleae were removed and placed in artificial perilymph (150 mM NaCl, 3.5 mM KCl, 1 mM CaCl_2 , 1 mM MgCl_2 , 2.75 mM Hepes and 2.25 mM Tris at $37\text{ }^\circ\text{C}$). The cochlea with the spiral ligament and stria vascularis were chipped away, containing the

ganglion spirale, afferent auditory fibers, axons, and axon terminals of the efferent bundles and the inner and outer hair cells, and some osseous and vascular structures.

In vitro microvolume superfusion:

The isolated cochleae were incubated for 35 min at 37 °C in 1 ml of the artificial perilymph containing 0.2 μM [7,8-³H]DA (specific activity: 45.0 Ci/mmol). Cochleae were then placed in plexi chambers (100 μl inside volume, three cochleae per chamber) and superfused with the artificial perilymph. After 1 h of preperfusion, the outflow was collected for 57 min in 3-min fractions and their DA content was determined by measuring the radioactivity of each sample. 0.5 ml aliquots of each sample were assayed with a liquid scintillation counter. After the collection period, cochleae were transferred to 0.5 ml of 10% trichloroacetic acid. Twenty-four hours later 0.1 ml was used to measure the radioactivity of the tissue. Electrical field stimulation was applied through platinum electrodes placed on top and bottom of the chambers during the 3rd (S1) and 13th fractions (S2) for 3 min at 30 V, 5 Hz, and 0.5 ms duration. Treatments were applied from the 21st minute of the collection period. NMDA was applied in the solution in the absence of Mg²⁺. In some cases the DA uptake blocker nomifensine was perfused from the beginning of the experiments. All perfusion solutions were continuously saturated with 100% O₂ and kept at 37 °C.

Data analysis:

The fractional release (FR) of the tritium-outflow was determined as the percentage of total radioactivity (³H-DA) that was present in the tissue at the time of the sample collection. The release evoked by the electrical field stimulations (S1 and S2), was determined as FRS1 and FRS2, i.e. the FR during S1 and S2 after subtracting the mean basal release. The effect of the study drug on the electrical stimulation-evoked release of [³H]DA was expressed as the ratio of FRS2/FRS1. The resting release was estimated by the calculation of the mean FR of DA within 6 min of the perfusion at three different periods (FRR1, 15–21 min; FRR2, 21–27 min; FRR3, 30–36 min). FRR2 and FRR3 were sampled in the presence of drugs but before

the second electrical stimulation, FRR1 corresponds to the control, drug-free period. The effect of drugs on the resting release was expressed by the ratio of the resting FR values in the presence of the drug (FRR2 or FRR3) over the value before the drug reached the preparation (FRR1) as FRR2/FRR1 or FRR3/FRR1. Experiments with different treatments were performed simultaneously in two microchambers. The data are expressed as mean \pm SEM. ANOVA followed by a Tukey post hoc comparison was used to determine the statistical significance.

4 RESULTS

Hemicochlea Ca^{2+} imaging

Ca^{2+} imaging of pillar, Deiters', and Hensen's cells in hearing mouse hemicochlea:

Cells were identified based on their anatomical location and shape under a 40x objective with red light oblique illumination. We determined the basal, resting $[\text{Ca}^{2+}]_i$ of the supporting cells in hearing mice at the beginning of every recording. Fig. 1B shows that the average resting $[\text{Ca}^{2+}]_i$ in the pillar (61 ± 4 nM, $n = 41$) and Deiters' cells (58 ± 5 nM, $n = 65$) was significantly lower than in the Hensen's cells (98 ± 10 nM, $n = 53$).

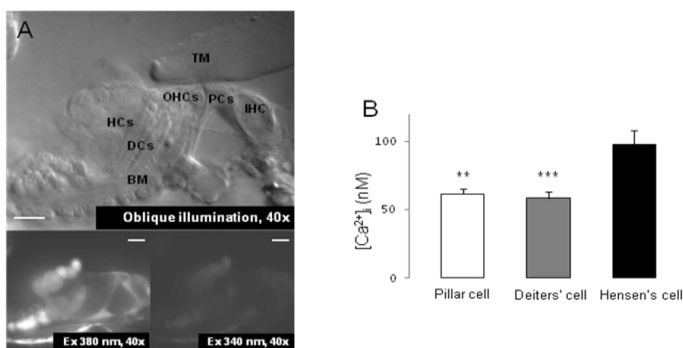


Fig. 1. Calcium imaging of the supporting cells in the hemicochlea preparation of hearing mice

A) Basal turn of the cochlea by oblique illumination, and fluorescent images at 340 and 380 nm excitation after bulk loading by fura-2 AM. TM, tectorial membrane; BM, basilar membrane; IHC, inner hair cell; PC, pillar cell; OHC, outer hair cell; DC, Deiters' cell; HC, Hensen's cell. Scale bars represent 20 μ m.

B) Basal $[Ca^{2+}]_i$ in different supporting cell types of the organ of Corti (n = 41, 65, 53; **p < 0.01; ***p < 0.001).

ATP evoked reversible and repeatable Ca^{2+} signals in the supporting cells in a dose-dependent manner:

ATP for 30 sec evoked characteristic, intracellular Ca^{2+} transients in a dose-dependent manner in all three types of supporting cells. The ATP responses were reversible and repeatable (Fig. 2A, upper traces). Pillar cells showed the lowest sensitivity for ATP vs. the Deiters' and Hensen's cells (Fig. 2A, bar graphs). Application of 50 μ M ATP induced a fast rising, uniformly shaped Ca^{2+} transient reliably in all three types of supporting cells ($\Delta[Ca^{2+}]_i$ in nM; pillar cells: 96 ± 14 nM, n=41; Deiters' cells: 104 ± 9 nM, n=65; Hensen's cells: 140 ± 10 nM, n=53), therefore we used this concentration of ATP in further experiments. Upon repeated application, the ATP response showed a reduction, in inverse correlation with the time interval between ATP administrations. There was no difference between the cell types in this respect (Fig. 2B, bar graphs). The reduction was negligible when the ATP applications followed each other by 20 min (pillar cells: 3 ± 16 %, n = 9; Deiters' cells: 6 ± 4 %, n = 14; Hensen's cells: 13 ± 4 %, n = 20; Fig. 2B, bar graphs).

ATP-evoked Ca^{2+} transients were mediated by Ca^{2+} influx and release of Ca^{2+} from internal stores in a cell-type specific manner

We tested the effect of ATP in Ca^{2+} -free buffer and after depletion of the SERCA-dependent intracellular Ca^{2+} stores. Ca^{2+} -free medium (+ 1 mM EGTA) suppressed the ATP-evoked intracellular Ca^{2+} signals significantly in all three types of cells (Fig. 3A and C). The inhibition was more pronounced in the Deiters' and the Hensen's cells (22 ± 8 and 22 ± 4 % of the 1st ATP response, respectively) compared to the pillar cells (38 ± 14 % of the 1st ATP response; Fig. 3C). The perfusion of the Ca^{2+} -free medium caused a modest decrease in basal $[Ca^{2+}]_i$ of 6 out of 7 (86 %) pillar, 3 out of 12 Deiters' (25 %) and 2 out of 14 Hensen's (14 %) cells.

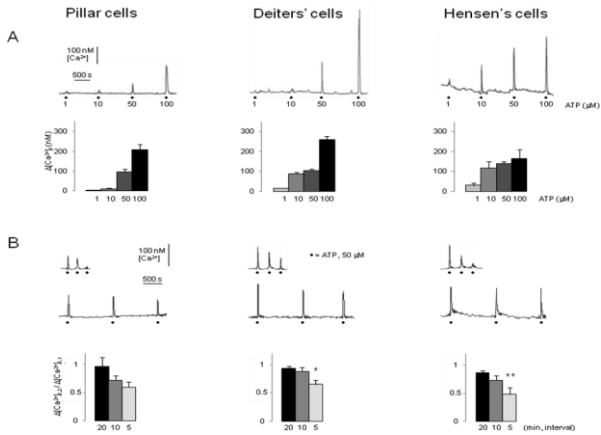


Fig. 2. ATP evoked reversible and repeatable intracellular Ca^{2+} transients in pillar, Deiters' and Hensen's cells

A) Upper traces: Black dots: ATP (1, 10, 50, 100 μM ; 30s); scale bars: $\Delta[Ca^{2+}]_i$ and time. Lower bar graphs: Mean $\Delta[Ca^{2+}]_i$ + SEM; Pillar cells, n = 4, 3, 41, 2; Deiters' cells, n = 9, 9, 65, 8; Hensen's cells, n = 2, 2, 53, 3.

B) Upper traces: Black dots: ATP (50 μM ; 30s); scale bars: $\Delta[Ca^{2+}]_i$ and time. Lower bar graphs: Mean ($\Delta[Ca^{2+}]_i,2 / \Delta[Ca^{2+}]_i,1$) + SEM; Pillar cells, n = 9, 6, 11; Deiters' cells, n = 14, 9, 20 and Hensen's cells, n = 20, 4, 8; *p < 0.05; **p < 0.01.

Emptying the ic. Ca^{2+} stores by the specific SERCA inhibitor CPA (10 μM) hampered the ATP-evoked transients significantly in all three cell types (Fig. 3B and C). Again, the effect was more robust in the Deiters' and Hensen's cells (18 ± 4 and 8 ± 3 % of the 1st ATP response, respectively) than in the pillar ones (33 ± 8 % of the 1st ATP response; Fig. 3C). CPA itself, before the 2nd ATP application, increased the $[Ca^{2+}]_i$ in all three cell types (Fig. 3B). There was a modest effect in pillar cells and more pronounced in Deiters' and Hensen's cells (Fig. 3D).

Both P2X and P2Y receptor subtype mRNAs were detected in the organ of Corti – PPADS revealed difference in the functional purinergic receptor population of pillar vs. Deiters' and Hensen's cells

We measured the mRNA expression of P2X and P2Y receptor subunits in the excised organ of Corti of P15-19 CD-1 mice. The RT-PCR analysis showed the presence of the mRNA of P2X2, P2X3, P2X4, P2X6, P2X7 and P2Y1, P2Y2, P2Y6, P2Y12, P2Y14 receptors in the whole organ of Corti (Fig. 4A).

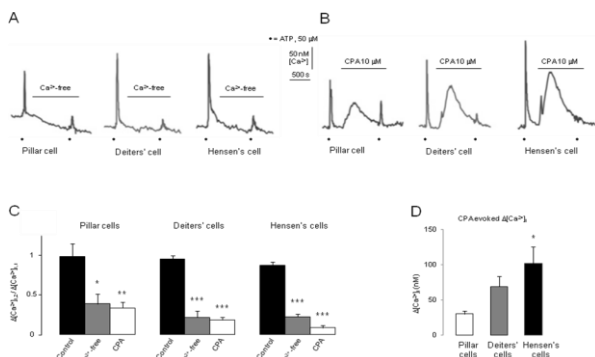


Fig. 3. ATP-evoked intracellular Ca²⁺ transients are extracellular Ca²⁺ and intracellular Ca²⁺ store dependent in the supporting cells of the organ of Corti

A-B) Black dots: ATP (50 μM; 30s); scale bars: Δ[Ca²⁺]_i and time; horizontal lines: Ca²⁺-free and CPA

C) Mean ($\Delta[Ca^{2+}]_i,2 / \Delta[Ca^{2+}]_i,1$) + SEM; Pillar cells, n = 9, 7, 8; Deiters' cells, n = 14, 12, 10 and Hensen's cells, n = 20, 14, 7. *p < 0.05; **p < 0.01, ***p < 0.001.

D) Mean Δ[Ca²⁺]_i + SEM; n = 8, 10, 7; *p < 0.05.

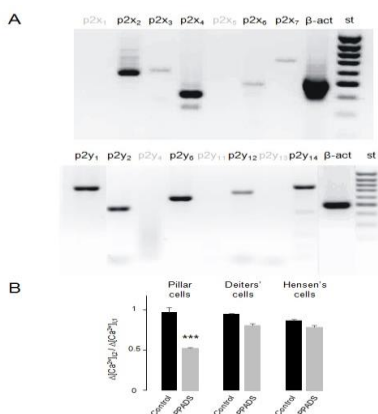


Fig. 4. RT-PCR analysis reveals the expression of multiple P2X and P2Y receptor subtypes in the organ of Corti of hearing mice. PPADS effect indicates different functional purinergic receptor population on pillar vs. Deiters' and Hensen's cells.

A) mRNAs encoding P2X2, P2X3, P2X4, P2X6, P2X7, and P2Y1, P2Y2, P2Y6, P2Y12, P2Y14 receptors (black letters) were present in the organ of Corti.

B) Mean ($\Delta[\text{Ca}^{2+}]_i,2 / \Delta[\text{Ca}^{2+}]_i,1$) + SEM; Pillar cells, n = 9, 9; Deiters' cells, n = 14, 14 and Hensen's cells, n = 20, 7; ***p < 0.001.

The widely used, broad-spectrum purinergic receptor antagonist PPADS (30 μM) inhibited the 50 μM ATP-evoked Ca^{2+} transients in the pillar cells, but did not influence them significantly in the Deiters' and Hensen's cells (Fig. 4B).

In vitro measurement of DA released from LOC terminals

Effect of NO on the DA release: the lack of endogenous tonic nitrenergic activity

To investigate the effect of NO on dopaminergic transmission, we applied the NO donor sodium nitroprusside in the perfusate. At a concentration of 300 μM , nitroprusside produced a large increase in the resting release of DA from isolated cochleae ($\text{FRR2}/\text{FRR1}=1.84^{\pm}0.10$; $P<0.001$). Nitroprusside failed to influence the stimulation-evoked release of DA ($\text{FRS2}/\text{FRS1}=1.13^{\pm}0.12$; $P<0.51$) (Fig. 5A–B). The selective NO donor DEA NONOate was applied at a 100 μM concentration. DEA NONOate also released DA from the isolated cochlea but the effect was smaller ($\text{FRR2}/\text{FRR1}=1.17^{\pm}0.03$; $P<0.01$; Fig. 5A–B). The inhibition of NOS by L-NAME (100 μM) did not influence the DA outflow ($\text{FRS2}/\text{FRS1}=1.05^{\pm}0.11$; $\text{FRR2}/\text{FRR1}=1.02^{\pm}0.06$), which indicated a lack of tonic NO release in this preparation (Fig. 5B).

NMDA-evoked NO production induces DA release

NMDA at 100 μM in Mg^{2+} -free solution and in the presence of glycine induced a relatively small, but highly significant release of DA at rest (n=12, Fig. 6A–B). We analyzed the resting release at the onset and a later phase of the perfusion (n=12, Fig. 6C). The increase in the resting release by 100 μM NMDA was significant at both phases ($\text{FRR2}/\text{FRR1}=1.12^{\pm}0.04$; $P<0.01$; $\text{FRR3}/\text{FRR1}=1.11^{\pm}0.04$; $P<0.001$). The DA mobilization by NMDA was not significantly

different between FRR3 and FRR2. NMDA also enhanced the electrically evoked DA release ($FRS_2/FRS_1=1.36\pm 0.09$; $n=10$, $P<0.05$; Fig. 6B). In a 10 μM concentration NMDA was ineffective to modulate the resting and electrical stimulation-evoked DA release (Fig. 6A).

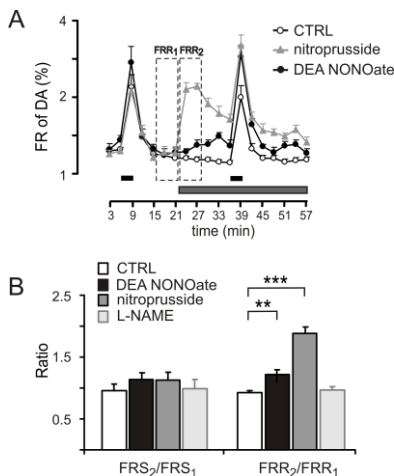


Fig. 5. Effect of exogenous NO and the lack of endogenous NO tone.

A) Nitroprusside sodium (300 μM), DEA NONOate (100 μM); horizontal black bars: electrical field stimulations (FRS1, FRS2); horizontal gray line: drug application

B) Nitroprusside sodium (300 μM), DEA NONOate (100 μM), L-NAME (100 μM); FRS₂/FRS₁: electrically evoked, FRR₂/FRR₁: resting outflow of DA; Mean \pm SEM; $n=8$, *** $P<0.001$; ** $P<0.01$

The releasing effect of NMDA was tested in the presence of L-NAME. L-NAME was perfused from the preperfusion and maintained until the end of the sample collection. At a low concentration (10 μM), L-NAME was ineffective in modulating NMDA-evoked DA release ($P<0.139$; Fig. 6D). The application of L-NAME at 100 μM caused a significant inhibition of the NMDA-evoked release of DA during the first phase of NMDA action ($FRR_2/FRR_1=0.99\pm 0.04$, $n=7$, $P<0.001$) but it left the later phase intact ($FRR_3/FRR_1=1.13\pm 0.06$, $n=7$, $P<0.879$) (Fig. 6C–D). The selective antagonist AP-5 was used in the bath at a 50 μM concentration from the preperfusion, that blocked the NMDA-evoked

increase in cochlear DA release (Fig. 6D). The NMDA was unable to enhance the electrically evoked release of DA.

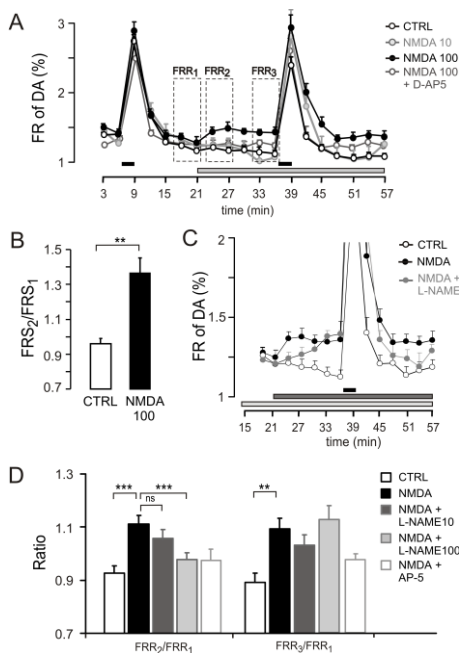


Fig. 4. NMDA receptors induce DA release in the cochlea through NO production.

A) NMDA (10, 100 μ M), D-AP-5 (50 μ M); horizontal black bars: electrical field stimulations (FRS₁, FRS₂); dashed rectangles: resting period (FRR₁), earlier phase of drug action (FRR₂), later phase of drug action (FRR₃); horizontal gray line: NMDA application

B) NMDA (100 μ M); mean + SEM; n=10, ** P<0.01.

C) NMDA (100 μ M), L-NAME (100 μ M); horizontal dark gray line: NMDA application; horizontal light gray line: L-NAME

D) L-NAME (10, 100 μ M), D-AP-5 (50 μ M); FRR₂/FRR₁: first phase of DA release, FRR₃/FRR₁: later phase of DA release; mean + SEM; n=10, ** P<0.01; * P<0.05.

Uptake is not involved in the action of NMDA

The presence of nomifensine did not influence the DA-releasing effect of NMDA (100 μ M; FRS₂/FRS₁=1.47 \pm 0.13; n=6, P<0.18, Fig. 7A–C). L-NAME (100 μ M) with nomifensine (10 μ M) also failed to influence the resting and stimulated DA outflow

(FRS2/FRS1=1.04[±]0.11;FRR2/FRR1=0.97[±]0.05, n=5, P<0.01, Fig. 7B–C).

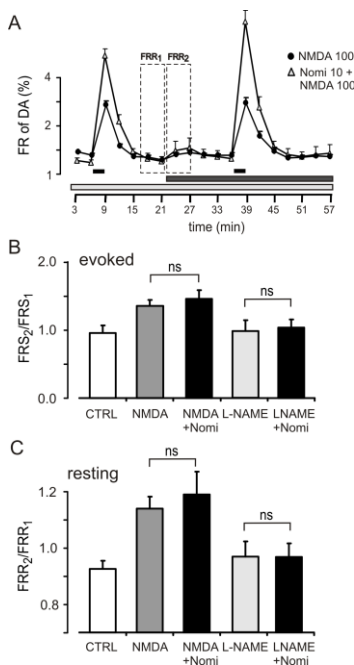


Fig. 5. Lack of effect of the uptake system to modulate the NMDA-evoked DA release
 A) gray triangles: NMDA (100 μ M) with nomifensine (10 μ M), solid circle: NMDA (100 μ M) without nomifensine; dark gray bar: NMDA application; light gray line: nomifensine application; horizontal black bars: electrical field stimulations (FRS1, FRS2)
 B) NMDA (100 μ M), L-NAME (100 μ M) without and with nomifensine (10 μ M); mean + SEM; ns: not significant.
 C) NMDA (100 μ M) and L-NAME (100 μ M) without and with nomifensine (10 μ M); means + SEM; ns: not significant (n=5–6).

4 DISCUSSION

Investigation of the ATP-regulated Ca^{2+} signaling is predominantly performed in isolated cells or cochlear explants from embryonic or newborn murines, experimental models which lacks normal tissue organization or contaminated by developmental biological factors. The advantage of our approach is that it allows the comparison of

calibrated $[Ca^{2+}]_i$ values of three different supporting cell types (pillar, Deiters' and Hensen's) investigated in the same in situ preparation from mature hearing mice. In our preparation, ATP evoked reversible and repeatable Ca^{2+} transients in a dose dependent manner in the 1–100 μ M range in all the investigated supporting cell types, and repeating the stimulus in 5 and 10 mins showed desensitization of the ATP response in all three cell types.

A straightforward way of separating the ionotropic P2X and the metabotropic P2Y receptor-mediated components of ATP-evoked Ca^{2+} responses from each other is withdrawing Ca^{2+} from the extracellular buffer and depleting intracellular Ca^{2+} stores by blocking their SERCA pump, respectively. In our experiments both intervention, omission of Ca^{2+} and application of CPA, inhibited the response, suggesting the involvement of both the ionotropic- and the metabotropic ATP receptors, in all three cell types. This conclusion, although without cell specificity and not on the protein level, was supported by the presence of the mRNA of P2X_{2,3,4,6,7} and P2Y_{1,2,6,12,14} receptors in the organ of Corti of the same preparation. Imaging experiments with a broad-spectrum purinergic antagonist PPADS provided further data regarding the functional expression of purinergic receptors in supporting cells. Its effect in pillar cells and the lack of its significant effect in Deiters' and Hensen's cells suggests involvement of distinct functional purinergic receptor populations in the ATP response in these cells.

The measurement of the effect of both Ca^{2+} withdrawal and depletion of endoplasmic reticulum (ER) Ca^{2+} stores on the ATP-evoked Ca^{2+} transients in pillar, Deiters' and Hensen's cells in the same study, especially in all three cell types in the same preparation, was not performed hitherto. We found that, besides the contribution of extracellular Ca^{2+} , the ATP-evoked Ca^{2+} transients were also dependent on the intracellular Ca^{2+} stores, but more strongly in the Deiters' and Hensen's cells than in the pillar ones. The more pronounced leak from the ER in Deiters', and especially in the Hensen's cells unmasked by the SERCA pump blocker CPA may also indicate the higher activity of the internal stores in Ca^{2+} signaling in these cells compared to the pillar ones. This may explain

the resistancy of basal $[Ca^{2+}]_i$ against Ca^{2+} withdrawal from the extracellular solution, which showed a reverse tendency, i.e., a decrease in $[Ca^{2+}]_i$ was observed with the highest prevalence in pillar and with the lowest one in Hensen's cells. The highest leak in Hensen's cells may also be related to the higher basal $[Ca^{2+}]_i$ of this cell type that could promote the loading of intracellular stores.

We observed supralinear additivity of the extracellular Ca^{2+} - and Ca^{2+} store-dependent ATP responses in Deiters' and Hensen's cells, versus the linear additivity in pillar cells, that suggests a synergistic interaction between the extracellular Ca^{2+} - and intracellular store-dependent ATP signaling in Deiters' and Hensen's cells. The interaction may reflect calcium-induced calcium release (CICR), and this might also explain the massive inhibitory effect of CPA, which seemed even more pronounced than that of the Ca^{2+} withdrawal. In CICR Ca^{2+} activates either ryanodine receptors or IP3 receptors that are Ca^{2+} channels of the internal stores. Traditionally, CICR is considered to phenomenon based on ryanodine receptors (RyRs), that has already been observed in the cochlea in hair cells and spiral ganglion neurons, but the role of RyR is controversial in the glia-like cochlear supporting cells. All these findings can be explained by age-dependency of RyR expression. IP3 was shown to be an important intercellular signaling molecule in the organ of Corti. Disturbances in its production impairs hearing. The IP3 receptor-dependent CICR is also in accordance with our findings of crucial involvement of internal Ca^{2+} stores and a CICR-like phenomenon in ATP-evoked Ca^{2+} signaling in the Deiters' and Hensen's cells.

In vitro measurement of DA released from LOC terminals

Although we found no evidence of tonic endogenous release, NO could effectively regulate the cochlear DA levels. NMDA receptor activation clearly increased the resting release of DA through NO production. It is possible that the NMDA receptors that are located outside of the cochlear dopaminergic system can contribute to the NO production and increase the resting DA release because NO is a diffusible transmitter. As a gaseous messenger molecule it is able to diffuse from any nearby cellular element equipped with NMDA

receptors. It is known that NMDA receptors are present in cochlea, especially on the inner and outer hair cell. NMDA receptor activation at these sites is likely to induce NO production; the released NO could diffuse to LOC terminals to increase the resting DA release.

We found that NO is produced in the early phase of NMDA receptor activation; the later phase of the NMDA action must be mediated by an unknown mechanism independent of DA uptake and NO. Our finding that NMDA application increased the resting DA release in the cochlea supports the idea that the glutamatergic transmission has a built-in protection system that prevents the connected elements from overactivation. This can be a local feedback mechanism within the organ of Corti: the excessive release of glutamate from the IHCs has the potential to decrease its own toxic effect by locally enhancing the release of DA, which protects the afferent nerve endings. The lack of the effect of nomifensine on the NMDA-evoked DA response, as found in our experiments, indicates that the NO-mediated component of NMDA action on DA release was most likely a result of NO diffusion and not a transporter-mediated action.

5 CONCLUSIONS

For the first time, we have performed functional ratiometric Ca^{2+} imaging (fura-2) in three different supporting cell types in the hemicochlea preparation of hearing mice to measure purinergic receptor-mediated Ca^{2+} signaling in pillar, Deiters' and Hensen's cells. ATP evoked reversible, repeatable and dose-dependent Ca^{2+} transients and desensitization in all three cell types. Involvement of both P2X and P2Y receptor types was proved in all three cell types. RT-PCR results supported this finding. The effect of the non-selective purinergic antagonist PPADS suggested different functional purinergic receptor population in pillar vs. Deiters' and Hensen's cells. We also found supralinear additivity of the extracellular Ca^{2+} -dependent P2X-mediated and the internal Ca^{2+} store-dependent P2Y-mediated ATP responses in the latter cell types, but not in the pillar cells, that might be explained by Ca^{2+} -induced Ca^{2+} release. This is in

accordance with the higher activity of the internal Ca^{2+} stores in Deiters' and Hensen's cells. These results might also reflect the distinct roles these cells play in cochlear protective function.

We showed that activation of NMDA receptors increased the electrical-field stimulation-evoked and the resting release of $[^3\text{H}]\text{DA}$ from the mouse cochlea. The initial phase of the resting DA release was NO mediated. We found no evidence of tonic endogenous release of NO and the inhibition of DA uptake was not involved in the paracrine NO effect. The Glu-evoked release of the protective DA might form the basis of an ultra-short local feed-back loop in the cochlea.

6 LIST OF PUBLICATIONS:

Publications used in the PhD thesis

Horváth T, Polony G, Fekete Á, Aller M, Halmos G, Lendvai B, Heinrich A, Sperlágh B, Vizi ES, Zelles T (2015). ATP-Evoked Intracellular Ca^{2+} Signaling of Different Supporting Cells in the Hearing Mouse Hemicochlea. **Neurochemical Research**, 41(1-2):364-75.

Halmos G, **Horváth T**, Polony G, Fekete Á, Kittel Á, Vizi ES, Van Der Laan BFAM, Zelles T, Lendvai B (2008). The role of N-methyl-D- aspartate receptors and nitric oxide in cochlear dopamine release. **Neuroscience**, 154(2), 796–803.

Other publications related to the Phd thesis

Polony G, Humli V, Andó R, Aller M, **Horváth T**, Harnos A, Tamás L, Vizi ES, Zelles T (2014). Protective effect of rasagiline in aminoglycoside ototoxicity. **Neuroscience**, 265:263-73.

Lendvai B, Halmos GB, Polony G., Kapocsi J, **Horvath T**, Aller M, Vizi ES, Zelles T (2011) Chemical neuroprotection in the cochlea:

The modulation of dopamine release from lateral olivocochlear efferents. **Neurochemistry International**, 59:(2) pp. 150- 158.

Halmos Gy, Doleviczényi Z, **Horváth T**, Polony G, Vizi E Szilveszter, Lendvai Balázs, Zelles T (2006) In vitro ischaemia hatása a cochlearis dopamin felszabadulására. **Fül- Orr- Gégegyógyászat**, 52:(4) pp. 245-252.

Other publications not related to the Phd thesis

Horváth T, Horváth B, Varga Z, Liktör B Jr, Szabadka H, Csákó L, Liktör B (2015) Severe neck infections that require wide external drainage: clinical analysis of 17 consecutive cases. **European archives of oto-rhino-laryngology**, 272(11) pp. 3469-74.

Horváth T (2011) Az információs forradalom orvosi szemmel. **Legge Artis Medicinae** 21(6-7) pp. 494-496